Research Square

Preprints are preliminary reports that have not undergone peer review.
They should not be considered conclusive, used to inform clinical practice,
or referenced by the media as validated information.

Disruption of Reelin signaling in a dual-hit mouse model of schizophrenia: impact of postnatal Δ9-tetrahydrocannabinol exposure in a maternal immune activation model

Benedicto Crespo-Facorro

bcrespo@us.es

Institute of Biomedicine of Seville / University of Seville

Celia Martín-Cuevas

Víctor Ramos-Herrero

Álvaro Flores-Martínez

Irene González-Recio

María Martínez-Chantar

Center for Cooperative Research in Biosciences (CIC bioGUNE) https://orcid.org/0000-0002-6446-9911

Juan C. Leza

Universidad Complutense de Madrid, Spain

J. Meana

University of the Basque Country UPV/EHU, CIBERSAM, Biocruces Health Research Institute https://orcid.org/0000-0002-7913-6714

Ana Sánchez-Hidalgo

Article

Keywords:

Posted Date: January 13th, 2026

DOI: https://doi.org/10.21203/rs.3.rs-7299003/v1

License: This work is licensed under a Creative Commons Attribution 4.0 International License.
Read Full License

Additional Declarations: The authors have declared there is **NO** conflict of interest to disclose

Version of Record: A version of this preprint was published at Translational Psychiatry on July 16th, 2026. See the published version at https://doi.org/10.1038/s41398-026-04282-1.

Abstract

Since the discovery of the first antipsychotic, pharmacological treatment of schizophrenia (SCZ) has primarily relied on agents that block D2 dopamine receptors. However, due to variability in patient responses, there is a pressing need to identify new biomarkers and therapeutic strategies. In this context, we have developed a dual-hit mouse model that combines maternal immune activation (MIA) induced by polyinosinic-polycytidylic acid (Poly(I:C)) and postnatal exposure to Δ9-tetrahydrocannabinol (THC), the psychoactive component of cannabis. We assessed the face validity of this model and investigated potential alterations in the Reelin signaling pathway. Our findings show a reduction in Reelin levels, a new potential key biomarker of SCZ, in the prefrontal cortex of male mice treated with THC compared to the dual-hit group, and across all treatment groups compared to controls in females. Additionally, a decrease in the number of Reelin + cells was observed across these groups. The dual-hit model exhibited phenotypes indicative of positive symptoms in males, as well as phenotypes associated with negative symptoms in both sexes. Furthermore, the model demonstrated reduced cortical thickness in THC-treated groups, alongside decreased dendritic spine density in both the prefrontal cortex and hippocampus in the dual-hit group.

1. Introduction

Since the discovery of the first antipsychotic, chlorpromazine, schizophrenia (SCZ) treatment has primarily targeted D2 dopamine receptors (1). However, patient responses vary widely; about 60% show significant improvement, while 30% remain resistant to standard therapies (2, 3). SCZ exhibits earlier onset, higher incidence and severity in men, indicating sexual dimorphism (4–7). This variability highlights the need to better understand the biological mechanisms underlying SCZ to develop more effective, targeted treatments.

SCZ is a chronic, severe psychiatric disorder with heterogeneous symptoms categorized as positive, negative, and cognitive (8–12). Both genetic and environmental factors, especially during prenatal stages, contribute to its etiology (13, 14). This has led to the neurodevelopmental hypothesis, which posits that prenatal and perinatal disturbances, genetic or environmental, interact with later factors to trigger disease onset during development (15).

Animal models enable controlled study of SCZ alterations, behavioral phenotypes, and therapeutic testing (7, 16). Most current models include only one type of alteration (genetic or environmental) and fail to reproduce the full spectrum of symptoms seen in the disorder. Therefore, combining multiple risk factors may more accurately replicate the clinical presentation of SCZ and further validate the hypothesis of neurodevelopmental disturbances. In light of this, the dual-hit hypothesis of SCZ has been proposed (17–20). This hypothesis suggests that a prenatal insult, such as an immune challenge during pregnancy leading to maternal immune activation (MIA), predisposes the individual to the development of SCZ (21–23), and a second postnatal insult further increases the risk, exceeding the threshold for the onset of the disorder (14, 24–27).

We developed a dual-hit mouse model to evaluate its validity and explore Reelin signaling. MIA was induced via polyinosinic-polycytidylic acid (Poly(I:C)) injection, a synthetic double-stranded RNA that triggers pro-inflammatory cytokine expression (28, 29). During adolescence, offspring received Δ9-tetrahydrocannabinol (THC), the psychoactive cannabis component that agonizes cannabinoid receptors CB1 and CB2 (17, 30). Cannabis use in adolescence increases SCZ risk (17, 31) and is linked to long-term cognitive deficits (13), cortical thinning (32), and reduced dendritic spine density and complexity in the prefrontal cortex (PFC) and hippocampus (HP) (33).

This dual-hit model provides a platform to identify SCZ therapeutic targets and advance treatment development. Reelin, an extracellular matrix (ECM) glycoprotein, has emerged as a promising SCZ biomarker (14, 34, 35). Reelin is crucial for neuronal migration and cortical layer formation during development (36), dendritic spine growth, synaptogenesis, synaptic plasticity (34, 37, 38), and adult neurogenesis (39).

Reelin binds apolipoprotein E receptor 2 (ApoER2) and very-low-density lipoprotein receptor (VLDLR), activating phosphorylation of Disabled homolog-1 (Dab1), an intracellular adaptor. Reelin includes a signal peptide, an F-spondin homology domain, a unique region, and a main body with eight repeats (R1–R8) plus a 33-amino acid basic extension (34, 36, 39, 40). Upon secretion, Reelin is cleaved at two sites, generating five fragments: N-R2, R3-6, R7-8, N-R6, and R3-8 (38, 41–43). Genetic alterations or decreased expression of Reelin and its signaling components have been documented in postmortem SCZ brains (35, 38, 44) and Alzheimer's Disease (AD), where such disruptions correlate with amyloid-beta accumulation and cognitive decline (45–47).

This study aims to investigate novel therapeutic targets for SCZ, focusing on validating Reelin as a potential biomarker within the context of a dual-hit model combining MIA and THC exposure (Fig. 1).

2. Methods

2.1 Animals

Adult C57BL/6J mice (8–10-weeks-old; Charles River Laboratories, France) were housed at the Instituto de Biomedicina de Sevilla (IBiS) in standard cages (max. 5 same-sex animals/cage) with corncob bedding and environmental enrichment under controlled conditions (22 ± 1°C; 12 h light/dark cycle, lights on at 8:00a.m.). Food and water were provided *ad libitum*. Mice were acclimated for 1–2 weeks before mating, in which one female was paired per cage with one male. Copulatory plugs were checked daily (GD0 = plug detection), and males were separated immediately thereafter. All procedures followed ARRIVE guidelines and were approved by the Institutional Animal Use Committee (13/10/2021/157).

2.2 Dual-hit model paradigm

2.2.1 Maternal Immune Activation

Poly(I:C) sodium salt (Sigma-Aldrich, #0000125513) was freshly dissolved in saline (1mg/ml) and administered intraperitoneally at 5mg/kg on GD9 to randomly assigned pregnant dams; controls received saline. Room temperature at the time of injection was 22 ± 1ºC. To minimize handling stress, dams received the injection in the same home cages where mating had previously taken place (9:00–10:00 a.m.) (Kentner et al., 2018). We selected GD9 due to its correspondence with a critical neurodevelopmental period in the mouse cortex, equivalent to the first/second trimester of human pregnancy (25, 48, 49) and a dose of 5mg/kg was chosen based on existing literature (25, 28, 50, 51). A single Poly(I:C) batch was used throughout to avoid inter-batch variability (52).

MIA induction was evaluated by monitoring maternal weight and temperature up to 48h-post-injection. At 3h, spleen and embryo/placenta samples were collected from a subset of dams (n = 2 per treatment) for cytokine analysis by RT-qPCR. Clinical signs of sickness behavior were monitored qualitatively. Weaning occurred at PD30. Offspring were housed by sex and litter (max. five per cage) with environmental enrichment. Both males and females were used in subsequent experiments. MIA validation is presented in Suppl. Fig. S1 and Suppl. Mat. 2.

2.2.2 THC exposure

THC (Sigma-Aldrich) was diluted in vehicle (5% ethanol, 5% cremophor, 90% saline) and administered intraperitoneally at 10 mg/kg once daily for six consecutive days during adolescence (PD55–60), modeling subchronic THC exposure. Offspring were randomly assigned to one of four experimental groups: Saline + Vehicle (control), Poly(I:C) + Vehicle, Saline + THC, and Poly(I:C) + THC (dual-hit). Body weight was monitored on PD55, PD60, and PD75 (n = 12–15 per group and sex; Suppl. Fig. S1).

2.3 Behavioral Assays

Behavioral testing was conducted between PD61–74 on 107 mice from the four experimental groups (Males: n = 14–15/group; Females: n = 12–14/group). One test was performed per day (9a.m.-5 p.m.) under dim lighting, from least to most stressful (Suppl. Fig. S2). All animals were assessed using the SHIRPA protocol (53). Mice were acclimated in the behavioral room for 30 min before the examination. Apparatuses were cleaned with 2% Derquim between subjects. Researchers conducting and analyzing behavioral tasks were blinded to treatment groups. Tests assessed phenotypes related to positive, negative, and cognitive symptoms (Suppl. Mat. 1.3 for protocols). Animals were sacrificed on PD75 by cervical dislocation or transcardial perfusion under thiobarbital anesthesia (Braun).

2.4 Biochemical analysis

PFC was dissected using a stainless brain matrix (Agnthos, 1mm) and snap-frozen in liquid nitrogen. Total protein was extracted from PFC across all experimental groups (n = 3–5 mice per group and sex). Tissue was lysed in 150–200 µl of lysis buffer, homogenized with a syringe, and centrifuged at 10,000–17,000 × g for 10 min at 4°C. Protein concentrations were determined using the BCA Protein Assay Kit (Thermofisher).

2.4.1 Proteomic analysis

Proteomic analysis was carried out in the Proteomic services at IBiS. Proteins were reduced and cysteine residues blocked with 50mM tris-(2-carboxyetyl) phosphine (TCEP, AB Sciex) and cloroacetamide (CAA, Sigma-Aldrich, St. Louis, MO, USA) for 30min at 37°C with shaking. Proteolysis was carried out at 37°C with trypsin (Promega, Fitchburg, WI, USA) at 1:20 (enzyme to substrate) at 37°C overnight with agitation. The resulting peptide samples were then quenched with formic acid (pH3) and desalted using a Stage-tip (Omix C18 tips, Agilent). Analysis of digested peptides was performed by LC-MS/MS with an Easy-nLC 1000 HPLC system (Thermofisher) coupled to a Q Exactive Plus Orbitrap mass spectrometer (Thermofisher). LC separations were performed on C18 HPLC precolumn (75µmx2cm) and Easy Spray HPLC column (75µmx25cm, 2µm, 100Å). Gradient elution was performed with a binary system consisting of (A) 0.1% aqueous formic acid and (B) 0.1% formic acid in CH3CN during 120min from 5–40% gradient of B with a flow rate of 250nl/min. A MS survey scan was obtained using a top 15 method with 100–2000m/z mass range. The MS/MS Spectra Acquisition was obtained using Higher-energy Collisional Dissociation (HCD). An isolation mass window of 2m/z was used for the precursor ion selection, and normalized collision energy of 27% was used for fragmentation. Ten second duration was used for the dynamic exclusion.

Protein was quantified by spectrometry-based label-free identification. Mass spectrometry data analysis was performed through Proteome Discoverer (Thermofisher) with search an Uniprot database for Mus Musculus with a false discovery rate (FDR) less than 1%. Ratios for each experimental group were calculated relative to the control group. The results were analyzed using Ingenuity Pathway Analysis (IPA) software (Qiagen).

2.4.2 Western blot

Equal amounts of protein (25–40 µg) were denatured by boiling in Laemmli buffer (5-10min) and separated by SDS-PAGE using 6–12% polyacrylamide gels. Proteins were transferred onto PVDF membranes (Millipore), blocked in 5% non-fat milk or BSA in TBS-T, and incubated with primary antibodies: mouse anti-Reelin (1:1000, MAB5364, Sigma-Aldrich), rabbit anti-Dab1 (1:500, #3328, Cell Signaling) or mouse anti-β-Actin (1:1000, A5316, Sigma-Aldrich). Immunoreactivity was detected using secondary antibodies conjugated with horseradish peroxidase (HRP) (1:5000): goat anti-mouse-HRP (NA931, Amersham) or donkey anti-rabbit-HRP (NA934, Amersham). Detection was performed using Clarity ECL Substrate (Bio-Rad) on a Chemidoc Touch Imaging System (Bio-Rad).

2.5 Histology

2.5.1 Immunofluorescence

Animals were perfused with PBS (n = 3–4 per group and sex). Brains were extracted, fixed overnight at 4 ºC in 4% PFA and immersed in 30% sucrose for 48 hours. Coronal sections of 25µm thickness were obtained using a cryostat (Leica). Sections were incubated in a sodium citrate solution, and blocked with

10% goat serum in PBS-T for 1h. Sections were incubated with mouse anti-Reelin (1:500, MAB5364, Sigma-Aldrich) and goat anti-mouse Alexa 594 (1:500, A-21203, Life Technologies), counterstained with DAPI and mounted on Superfrost-Plus slides with DAKO (Agilent). Images were acquired in a Thunder microscope (Leica, 20x objective) and analyzed using the ImageJ software. Density of Reelin + cells was automatically quantified using a minimum of 4 slices per mice, averaging three randomly selected fields within the prelimbic area. Cortical thickness measurement was carried manually out using the DAPI staining in the primary somatosensory area.

2.5.2 Golgi-Cox staining

Golgi-Cox staining was performed as described previously (54). Animals were anesthetized, decapitated, and the brains were extracted and hemisected (n = 5–16 per group). The hemispheres were immersed in Golgi-Cox solution for 3 weeks. Coronal sections of 200µm were cut using a vibratome (Leica) and incubated with 14–16% ammonium hydroxide (1h). Sections were then treated with sodium thiosulfate (7min), dehydrated through an ethanol series (50–100%) and cleared with xylene. Sections were mounted in Superfrost-Plus slides with DPX. Z-stacks images of a 0.75µm step size were acquired in a BX-61 bright-field microscope (Olympus, 100x objective). Dendritic spines were manually counted using ImageJ software and spine density was averaged for each neuron.

2.6 RT-qPCR

Total RNA was extracted from homogenized maternal spleen or embryos (with placenta) with the RNeasy mini kit (Qiagen). For each sample (n = 2 dams and n = 6 embryos per group), 1µg of total RNA was used for reverse transcription to cDNA (qScript cDNA supermix, Quantabio). qPCR was performed with iTaq Universal Probes Supermix (Bio-Rad) and Taqman probes (IL-6: Mm00446190_m1; TNFα: Mm900443258_m1; GADPH: Mm99999915_g1, Thermofisher Scientific) on a ViiA 7 Real-Time PCR system (Thermofisher). Each sample was analyzed in duplicate.

2.7 Statistical analysis

Data are presented as the mean ± standard error of the mean (SEM). Statistical procedures were performed using GraphPad Prism™ 8 software (San Diego, CA, USA). Significance was defined as $p < 0.05$. Appropriate statistical tests, including three-way and two-way ANOVAs, and unpaired Student's t-test, were performed. Post-hoc multiple comparisons were carried out using Tukey's or Sidak's correction, as applicable.

3. Results

3.1 Behavioral characterization of the dual-hit model

3.1.1 Dual-hit male mice exhibit enhanced stereotyped behavior

The effects of prenatal Poly(I:C) and postnatal THC on locomotion and anxiety were evaluated using the open field test. While THC does not affect these parameters after an extended drug-free period (55, 56), acute THC exposure can alter anxiety and locomotion in mice (56). A three-way ANOVA revealed significant main effects of sex and THC on both the total distance traveled (Sex: $F(1, 99) = 6.069$, $p < 0.05$; THC: $F(1, 99) = 14.21$, $p < 0.001$) and the mean velocity (Sex: $F(1, 99) = 6.142$, $p < 0.05$; THC: $F(1, 99) = 14.51$, $p < 0.001$) (Fig. 2A). In male mice, a two-way ANOVA revealed a significant main effect of THC on both the total distance traveled ($F(1, 52) = 10.27$, $p < 0.01$) and the mean velocity ($F(1, 52) = 10.39$, $p < 0.01$). Post-hoc comparisons showed that Saline + THC group exhibited reduced locomotor activity and mean velocity compared to Poly(I:C) + Vehicle group ($p < 0.05$). Similarly, Poly(I:C) + THC group also displayed a significant decrease in mean velocity relative to Poly(I:C) + Vehicle group ($p < 0.05$). Additionally, there was a trend toward decreased distance traveled in Poly(I:C) + THC compared to Poly(I:C) + Vehicle ($p = 0.051$). In female mice, a two-way ANOVA revealed a significant main effect of THC on both total distance traveled ($F(1, 47) = 5.363$, $p < 0.05$) and mean velocity ($F(1, 47) = 5.516$, $p < 0.05$). Although post-hoc analyses did not detect statistically significant pairwise differences between groups, a general reduction in locomotor activity was observed in THC-treated groups. Overall, these findings suggest that THC impairs locomotion regardless of prior immune activation, although the combination with Poly(I:C) may exacerbate the effect.

Also regarding positive symptoms, the self-grooming test was used to study stereotyped behavior (57). Several MIA models have reported an increased grooming time (28, 58, 59). A three-way ANOVA revealed a significant effect of Poly(I:C) ($F(1, 90) = 4.183$, $p < 0.05$) and a trend toward an interaction effect of Poly(I:C) x THC ($p = 0.070$) (Fig. 2B). In males, a two-way ANOVA showed significant effects of both THC ($F(1, 49) = 7.196$, $p < 0.01$) and Poly(I:C) ($F(1, 49) = 4.361$, $p < 0.05$). Post-hoc analyses indicated increased grooming time in the Poly(I:C) + THC group compared to controls ($p < 0.01$) and Poly(I:C) + Vehicle mice ($p < 0.05$). Additionally, there was a trend toward increased grooming time in Poly(I:C) + THC group compared to Saline + THC group ($p = 0.063$). In females, no significant differences were observed in the two-way ANOVA. These results indicate that the combination of Poly(I:C) and THC exerts a synergistic effect on self-grooming time in males.

On the other hand, cannabis exposure affects motor learning and performance (60) as well as movement speed and balance (61). In the rotarod test, a repeated-measures three-way ANOVA revealed a significant main effect of day ($F(1.63, 84.93) = 41.32$, $p < 0.0001$) and a significant day × Poly(I:C) x THC interaction ($F(2, 104) = 4.193$, $p < 0.05$). Post-hoc comparisons showed a general trend of improved motor performance in all treatment groups, reflected by increased latency to fall compared to control animals (Fig. 2C). In female mice, the analysis revealed a significant main effect of day ($F(1.81, 85.12) = 47.44$, $p < 0.0001$) and day x THC interaction ($F(2, 94) = 6.736$, $p < 0.01$). However, post-hoc comparisons did not detect statistically significant differences between treatment groups at any individual time point.

There were no significant differences between groups or sexes in heat sensitivity (hotplate) (suppl. Fig. S3). In the startle reflex and prepulse inhibition test, a main effect of stimulus intensity was observed in both the prepulse inhibition phase ($F(1.47, 47.08) = 33.02$, $p < 0.0001$) and the acoustic startle response

phase ($F(2.33, 74.53) = 169.2$, $p < 0.0001$). However, no main effects of Poly(I:C), THC or their interaction were detected (suppl. Fig. S4).

3.1.4 The dual-hit model impairs social novelty in both sexes and reduces dominance in male mice

SCZ patients display negative symptoms such as social withdrawal and anhedonia (33) which are modeled in animals through social tests. In the social preference phase of the three-chamber test, no significant effects were detected in the three-way ANOVA in the social index (Fig. 3A). However, in the social novelty phase, the analysis showed significant main effects of both Poly(I:C) ($F(1, 99) = 7.125$, $p < 0.01$) and THC ($F(1, 99) = 11.39$, $p < 0.01$) in the memory index (Fig. 3B). As sex showed no significant main effect, data were pooled across sexes. A two-way ANOVA revealed significant main effects of both prenatal Poly(I:C) ($F(1, 103) = 7.482$, $p < 0.01$) and postnatal THC ($F(1, 103) = 11.86$, $p < 0.001$) on the memory index. Post-hoc analysis showed a significant reduction in the memory index in the Poly(I:C) + THC group compared to controls ($p < 0.001$), as well as in the Saline + THC group ($p < 0.01$) and the Poly(I:C) + Vehicle group ($p < 0.05$), indicating that both treatments independently and additively impaired recognition memory performance.

Regarding social dominance, a three way ANOVA revealed a significant main effect of THC on the percentage of wins in the tube test ($F(1, 90) = 13.98$, $p < 0.001$), as well as a significant sex x Poly(I:C) interaction ($F(1, 90) = 14.42$, $p < 0.001$) (Fig. 3C). Analysis of paired treatments is available in suppl. Fig. S5. In male mice, a two-way ANOVA showed a significant main effect of Poly(I:C) on the percentage of wins ($F(1, 49) = 4.483$, $p < 0.05$), along with a trend toward a main effect of THC ($p = 0.058$). Post-hoc comparisons showed that Poly(I:C) + THC male mice displayed a significantly lower proportion of wins compared to controls ($p < 0.05$) and Saline + THC animals ($p < 0.05$). Additionally, a trend toward reduced dominance was observed when comparing Poly(I:C) + THC males to Poly(I:C) + Vehicle animals ($p = 0.077$), suggesting a potential synergistic effect of the two exposures on social dominance behavior. Regarding females, a two-way ANOVA revealed significant main effects of both Poly(I:C) ($F(1, 41) = 10.01$, $p < 0.01$) and THC ($F(1, 41) = 10.49$, $p < 0.01$). Post-hoc comparisons showed that Saline + THC females exhibited a significantly lower proportion of wins compared to the Poly(I:C) + Vehicle group ($p < 0.001$). Additionally, there was a trend toward reduced dominance in the Saline + THC group compared to both the controls ($p = 0.079$) and the Poly(I:C) + THC group ($p = 0.072$), suggesting that THC alone may impair social dominance behavior in females, independently of MIA.

3.1.6 Poly(I:C) alone impairs recognition memory in female mice

THC exposure in rodent models causes short-term recognition memory alterations (32, 62), as well as prenatal Poly(I:C) infection (29, 63, 64). In the novel object recognition test, regarding the memory index, a three-way ANOVA revealed a significant main effect of Poly(I:C) ($F(1, 78) = 8.708$, $p < 0.01$), and sex x THC interaction ($F(1, 78) = 5.139$, $p < 0.05$). In males, a two-way ANOVA showed no significant differences between groups. However, in females, there was a main effect of Poly(I:C) ($F(1, 36) = 6.467$,

$p < 0.05$) and THC ($F(1, 36) = 8.294$, $p < 0.01$). Post-hoc analysis revealed a reduced memory index in Poly(I:C) + Vehicle mice compared to controls ($p < 0.05$), Saline + THC ($p < 0.01$) and Poly(I:C) + THC ($p < 0.05$) mice (Fig. 3D). There were no differences in the y-maze test (suppl. Fig. S6). These findings suggest that Poly(I:C) selectively impairs object recognition memory in female mice, while no significant effects were observed in males.

3.2 The Reelin pathway is altered in dual-hit mice

3.2.1 Proteomic analysis

PFC samples (n = 4–5 per treatment and sex) were analyzed using label-free quantitative proteomics (Fig. 4). The raw data from this analysis is available as Supplemental Data (suppl. mat. 3). This analysis served to identify proteins significantly altered in dual-hit male and female mice (Fig. 4A, B). A total of 375 altered proteins were detected in male mice and 447 in female mice compared to controls (Fig. 4A).

Notably, 113 proteins were common to both conditions, suggesting a core set of proteins consistently expressed under the dual-hit paradigm. Furthermore, 262 proteins were uniquely altered to male mice, while 334 were exclusive to females (the list of altered proteins in males, females, and common to both is available in suppl. mat. 4). These findings indicate a sex-specific protein signature of the dual-hit paradigm and highlight potential therapeutic targets for further investigation. A higher proportion of altered proteins was observed in female dual-hit mice compared to their controls (Fig. 4B). These results suggest that the dual-hit paradigm induces a more extensive protein expression response in females than in males, highlighting potential sex-specific mechanisms underlying this condition. A similar pattern was also observed in the analysis of altered canonical pathways, showing a higher number in female dual-hit mice compared to their controls and Saline + THC male mice (Fig. 4C). The 30 most significantly altered canonical pathways between the dual-hit groups and their respective controls are shown in Fig. 4D. Among the pathways most relevant to SCZ, significant alterations were observed in interleukin (IL) signaling -specifically IL-1, IL-2, IL-3, IL-8, IL-12 and IL-17A- as well as in synaptogenesis, axonal guidance, actin cytoskeleton and integrin signaling, long term depression, and glutamatergic, GABAergic, and dopamine receptor pathways (Fig. 4E). Notably, the Reelin pathway in neurons emerged as particularly noteworthy due to its relevance in SCZ. This pathway was significantly altered in Saline + THC males compared to their controls (suppl. Fig. S7), and across all treatment groups (Poly(I:C) + Vehicle, Saline + THC y Poly(I:C) + THC) when compared to their respective female controls, highlighting its potential role within the dual-hit paradigm. Similar results were observed in the analysis comparing Saline + THC and control mice (suppl. Fig. S6). Briefly, a total of 293 proteins were found to be altered uniquely in male Saline + THC mice, and 303 in female mice, with 91 altered proteins common to both groups. The most significantly altered canonical pathways were associated with GABAergic and glutamatergic signaling, Reelin signaling in neurons, as well as ILK, actin cytoskeleton, IL-2, and integrin signaling.

3.2.2 Reelin and Dab1 expression levels

The alteration in the Reelin pathway was confirmed via Western blot analysis in PFC samples by evaluating the expression levels of Reelin, its N-R2 fragment and Dab1 (Fig. 5A). Regarding Reelin expression, a three-way ANOVA reveled a significant main effect of sex ($F(1, 16) = 5.408$, $p < 0.05$), and Poly(I:C) x THC interaction ($F(1, 16) = 10.21$, $p < 0.01$). Additionally, there were trends toward significance for the main effects of THC ($p = 0.051$) and Poly(I:C) ($p = 0.072$). In males, the analysis showed a main effect of Poly(I:C) ($F(1, 8) = 10.07$, $p < 0.05$) and Poly(I:C) x THC interaction ($F(1, 8) = 13.27$, $p < 0.01$) (Fig. 5B). Post-hoc analysis reported that Reelin expression was decreased in Saline + THC male mice compared to the dual-hit group ($p < 0.01$). In females, a two-way ANOVA revealed a trend toward a main effect of postnatal THC treatment ($p = 0.051$) (Fig. 5C). Although post-hoc comparisons did not reach statistical significance, THC-exposed groups showed a general reduction in Reelin expression compared to controls.

Regarding N-R2 fragment, a three-way ANOVA reported significant main effects of sex ($F(1, 16) = 5.542$, $p < 0.05$) and THC ($F(1, 16) = 9.872$, $p < 0.01$). Additionally, a trend toward a Poly(I:C) x THC interaction was observed ($p = 0.077$), suggesting a possible combined influence of prenatal and postnatal hits. In males, there was a main effect of THC ($F(1, 8) = 5.934$, $p < 0.05$) (Fig. 5B). However, post-hoc comparisons did not identify significant pairwise differences between groups. Despite this, a general reduction in N-R2 expression level was observed across both THC-treated groups compared to controls. In females, a two-way ANOVA revealed a trend toward a main effect of THC ($p = 0.059$) (Fig. 5C). Although post-hoc comparisons did not reach statistical significance, a consistent pattern of reduced N-R2 expression was observed across all treated groups compared to controls. Therefore, a reduction in both full-length Reelin and its N-R2 fragment levels was observed, rather than an accumulation of the fragment. This suggests that the decrease in Reelin expression is unlikely to be attributed to enhanced proteolytic processing of its N-terminal region.

With respect to Dab1, a three-way ANOVA revealed significant main effects of sex ($F(1, 16) = 15.51$, $p < 0.01$) and THC ($F(1, 16) = 10.05$, $p < 0.01$), as well as a significant sex x THC interaction ($F(1, 16) = 18.20$, $p < 0.001$). In males, a two-way ANOVA did not show any effects (Fig. 5B). However, in females, there was a main effect of THC ($F(1, 8) = 16.17$, $p < 0.01$), and post-hoc analysis revealed an increased Dab1 expression in dual-hit mice compared to controls ($p < 0.05$) and Poly(I:C) + Vehicle mice ($p < 0.05$) (Fig. 5C). Dab1 expression has been utilized as an indicator of Reelin signaling activity, given that Reelin binding to its receptors triggers Dab1 phosphorylation (Ogino et al., 2017). Therefore, the observed increase in Dab1 levels is consistent with the reduction in Reelin expression.

In summary, the non-significant reduction in expression levels of both Reelin and its N-R2 fragment in the Saline + THC group in males, and across all three experimental groups in females, and the significantly altered Dab1 expression levels in females, collectively support the disruption of the Reelin pathway observed in the proteomic study.

3.2.3 Reelin + cell density is reduced in dual-hit female mice

The density of Reelin + cells in the prelimbic area of PFC was quantified. A three-way ANOVA revealed significant main effects of sex ($F(1, 23) = 14.49$, $p < 0.001$) and THC ($F(1, 23) = 19.71$, $p < 0.001$), as well as a significant sex x Poly(I:C) interaction ($F(1, 23) = 7.017$, $p < 0.05$). Additionally, a trend toward a three-way interaction (sex x Poly(I:C) x THC) was observed ($p = 0.079$).

In male mice, there was a main effect of THC ($F(1, 12) = 5.534$, $p < 0.05$), and post-hoc analysis showed a non-significant decrease in the Saline + THC mice compared to controls ($p = 0.087$). In female mice, there was a main effect of both Poly(I:C) ($F(1, 11) = 9.899$, $p < 0.01$) and THC ($F(1, 11) = 16.30$, $p < 0.01$), and post-hoc analysis revealed a reduction in Poly(I:C) + THC compared to controls ($p < 0.01$) and Poly(I:C) treatment alone ($p < 0.05$). Moreover, the dual-hit group showed a marginally significant decrease in Reelin + cell density compared to Saline + THC group ($p = 0.053$) (Fig. 5D). These results are consistent with the findings from the Western blot experiments, as a reduced density of Reelin + cells was observed in the same groups where the lower expression levels of Reelin protein were detected.

3.3 Cortical thickness is reduced by THC exposure

SCZ patients exhibit reduced cortical thickness across several brain regions, such as PFC (65, 66). Similarly, MIA models also show alterations in cortical thickness (67, 68, 21, 69). Additionally, cannabis use can impact cortical thickness in SCZ patients (70–72). Since no significant effects of sex were detected in the three-way ANOVA, data from both sexes were combined. A two-way ANOVA revealed a significant effect of THC in total cortical thickness ($F(1, 33) = 15.33$, $p < 0.001$). Post-hoc analysis reported a significant reduction in Saline + THC mice compared to controls ($p < 0.05$) and Poly(I:C) + Vehicle ($p < 0.01$). Poly(I:C) + THC showed a non-significant reduction in total cortex compared to Poly(I:C) alone ($p = 0.058$). THC also showed a significant effect when cortical layers were analyzed separately, specifically in layer IV ($F(1, 33) = 17.23$, $p < 0.001$). Post-hoc analysis revealed a reduction in layer IV in Saline + THC mice compared to controls ($p < 0.05$) and Poly(I:C) + Vehicle ($p < 0.01$). Dual-hit mice also showed a reduction compared to Poly(I:C) + Vehicle ($p < 0.05$) (Fig. 6A). Taken together, the results suggest that postnatal THC exposure is the main factor contributing to the reduction in cortical thickness. Although the effect in the dual-hit group did not reach significance, a similar trend was noted.

3.4 Poly(I:C) + THC combination decreases dendritic spine density in PFC and HP

As sex showed no significant effect in the three-way ANOVA, data were pooled across sexes. In the CA1 region of the HP, the main effect of Poly(I:C) was observed on dendritic spine density ($F(1, 36) = 9.514$, $p < 0.01$). Post-hoc analysis indicated a significant reduction in dual-hit group compared to controls ($p < 0.05$) (Fig. 6B). In PFC, a significant effect of Poly(I:C) was found ($F(1, 36) = 16.47$, $p < 0.001$). Post-hoc analysis revealed a significant decrease in spine density in the Poly(I:C) + Vehicle ($p < 0.01$) and dual-hit ($p < 0.01$) groups compared to controls (Fig. 6C). Overall, these results indicate that dendritic spine density is affected by the initial impact and is significantly further influenced by postnatal THC exposure.

4. Discussion

We established a dual-hit model showing alterations in Reelin signaling, suggesting Reelin as a potential biomarker for SCZ and supporting the dual-hit hypothesis. Behavioral phenotypes linked to positive symptoms appeared in males and negative symptoms in both sexes. THC led to reduced cortical thickness and dendritic spine density. Offspring viability was not affected, and MIA was confirmed in all dams. Both sexes were included to assess sexual dimorphism (73). We observed sex differences in behavior, proteomics, and Reelin pathway alterations.

Poly(I:C)-exposed models show altered stereotyped and social behavior, memory, cognitive flexibility, and anxiety (74, 75). Our behavioral tests revealed altered social behavior and stereotypy in dual-hit mice, consistent with adolescence as a critical period for cannabis-induced symptoms (33). Locomotor alterations likely reflect acute THC effects, as the open field test occurred 24 hours after the last injection (56). Poly(I:C) + THC males exhibited reduced dominance, an effect not seen in females, possibly due to higher baseline male dominance making changes more detectable (76–79). No significant cognitive impairments were observed, possibly due to early Poly(I:C) administration (GD9) (33, 80), since later exposure causes more severe deficits linked to GABAergic system development (80).

Proteomic analyses revealed significant alterations in the Reelin pathway across most treatment comparisons, especially in females. Notably, Reelin was overexpressed in the dual-hit group rather than reduced, differing from models showing Reelin downregulation after prenatal insults. This may reflect long-term modifications in the endocannabinoid system induced by prenatal Poly(I:C), modulated by THC exposure, though further study is needed (24). Females showed a non-significant trend toward decreased Reelin, suggesting THC influences Reelin expression more than prenatal Poly(I:C). The reduction in Reelin was hypothesized to result from increased N-terminal proteolytic cleavage causing N-R2 fragment accumulation (41, 42, 81). However, N-R2 expression mirrored full-length Reelin, ruling out this mechanism. Dab1, whose phosphorylation indicates Reelin receptor activation, was measured to infer signaling potency (40). Dab1 levels were unchanged in males but significantly increased in dual-hit females compared to controls and Poly(I:C) alone, supporting disruption of the Reelin pathway consistent with reduced Reelin levels.

The neurobiological interplay between MIA and THC remains incompletely understood. Prior work suggests convergent mechanisms involving neuron-microglia-astrocyte communication in response to dual insults (26). We extend this view by proposing ECM, particularly Reelin's role in neuron-glia interactions, as a key convergent factor within the dual-hit hypothesis (14).

Reduced cortical thickness has been consistently reported in SCZ patients (65, 66) individuals with chronic cannabis use (71). Our model showed similar cortical thinning in THC-treated groups. Further studies quantifying neuronal density are needed to determine if thinning reflects neurodegeneration, cell loss, or other causes. Additionally, reduced dendritic spine density, a hallmark of SCZ (82) was evident in dual-hit mice. Reelin secretion during prenatal stages primarily originates from Cajal-Retzius cells in the

cortical marginal zone (38, 43). The dendritic spine impairments likely result from decreased Reelin expression in these cells due to Poly(I:C), further exacerbated by THC exposure (40).

Several limitations must be noted. First, focusing on PFC limits generalization to other brain regions. Second, mouse models, while controlled, cannot fully capture SCZ complexity. Third, additional behavioral tests for fear conditioning, spatial learning, and anxiety would broaden phenotyping. Lastly, THC dosage and administration route affect outcomes; exploring inhalation or other delivery methods could improve translational relevance. These factors should be considered when interpreting results.

In conclusion, we developed a dual-hit model combining Poly(I:C) with THC exposure. Male dual-hit mice displayed stereotyped behavior and social deficits consistent with positive and negative SCZ symptoms, while females showed social impairments. THC exposure led to reduced Reelin expression and N-R2 fragment in PFC, especially in females, along with decreased Reelin + cell density and increased Dab1 levels, indicating adolescent THC primarily drives Reelin signaling disruption. THC also caused cortical thinning, and dual-hit mice showed reduced dendritic spine density in PFC and HP. This paradigm is a valid model for investigating the dual-hit hypothesis in SCZ, highlighting Reelin as a potential biomarker.

Abbreviations

Δ9-tetrahydrocannabinol (THC), Alzheimer's Disease (AD), apolipoprotein E receptor 2 (ApoER2), disabled homolog-1 (Dab1), endocannabinoid receptors (CBR), extracellular matrix (ECM), gestational day (GD), hippocampus (HP), Ingenuity Pathway Analysis (IPA), maternal immune activation (MIA), polyinosinic-polycytidylic acid (Poly(I:C)), prefrontal cortex (PFC), postnatal day (PD), schizophrenia (SCZ), very low-density lipoprotein receptor (VLDLR).

Declarations

Declaration of Competing Interest

The authors declare that they have no competing financial interests or personal relationships that could have influenced the work reported in this article.

Acknowledgements

This work was supported by the Consejería de Conocimiento y Universidades through project PID2019-109405RB-I00/AEI/10.13039/501100011033; the Andalusian Plan for Research, Development, and Innovation and ERDF/EU through project P20_00811; the Regional Ministry of Health (Junta de Andalucía) through project PI-0014-2022; the Instituto de Salud Carlos III (ISCIII) co-funded by the European Union, through projects AC23_2/00034 and PI22/01379, and unrestricted research funding from the Spanish Network for Research in Mental Health (CIBERSAM, G26). CM-C was supported by CIBERSAM (G26) and the Instituto de Salud Carlos III (AC23_2/00034) and VDR-H by the Agencia Estatal de Investigación (PID2019-109405R and PI-0014-2022). AF-M, IG-R, MLM-C, JCL and JJM were

supported by their affiliations. BC-F received unrestricted research funding from Instituto de Salud Carlos III, MINECO, Gobierno de Cantabria, Spanish Network for Research in Mental Health (CIBERSAM), from the Seventh European Union Framework Program and Lundbeck. He has also received honoraria for his participation as a consultant and/or as a speaker at educational events from Janssen Johnson and Johnson, Mylan, Lundbeck, and Otsuka Pharmaceuticals. ACS-H received funding from CIBERSAM (G26) and from the Consejería de Salud y Familias (RH-0063).

Authors contributions

CM-C contributed to investigation, conceptualization, writing of the original draft, and writing, reviewing, and editing of the manuscript. VDR-H was responsible for investigation, formal analysis, and methodology. AF-M contributed to formal analysis, methodology, and writing of the original draft, as well as writing, reviewing, and editing of the manuscript. IG-R and MLM-C participated in formal analysis. JCL contributed to conceptualization. JJM was involved in conceptualization and methodology. BC-F contributed to conceptualization and oversaw funding acquisition, project administration, supervision, writing, reviewing, and editing of the manuscript. ACS-H contributed to conceptualization, investigation, supervision, writing of the original draft, and writing, reviewing, and editing of the manuscript. All authors have read and approved the final version of the manuscript.

References

1. Carlsson A, Carlsson ML. A dopaminergic deficit hypothesis of schizophrenia: the path to discovery. Dialogues in Clinical Neuroscience. 2006;8(1):137–42.
2. Crespo-Facorro B, Pelayo-Terán JM, Pérez-Iglesias R, Ramírez-Bonilla M, Martínez-García O, Pardo-García G, et al. Predictors of acute treatment response in patients with a first episode of non-affective psychosis: Sociodemographics, premorbid and clinical variables. Journal of Psychiatric Research. 2007;41(8):659–66.
3. Moreno-Sancho L, Juncal-Ruiz M, Vázquez-Bourgon J, Ortiz-Garcia De La Foz V, Mayoral-van Son J, Tordesillas-Gutierrez D, et al. Naturalistic study on the use of clozapine in the early phases of non-affective psychosis: A 10-year follow-up study in the PAFIP-10 cohort. Journal of Psychiatric Research. 2022;153:292–9.
4. Aleman A, Kahn RS, Selten JP. Sex Differences in the Risk of Schizophrenia: Evidence From Meta-analysis. Arch Gen Psychiatry. 2003;60(6):565.
5. Eranti SV, MacCabe JH, Bundy H, Murray RM. Gender difference in age at onset of schizophrenia: a meta-analysis. Psychol Med. 2013;43(1):155–67.
6. Mendrek A, Mancini-Marïe A. Sex/gender differences in the brain and cognition in schizophrenia. Neuroscience & Biobehavioral Reviews. 2016;67:57–78.
7. Shangase KB, Luvuno M, Mabandla MV. Investigating the Robustness of a Rodent “Double Hit” (Post-Weaning Social Isolation and NMDA Receptor Antagonist) Model as an Animal Model for Schizophrenia: A Systematic Review. Brain Sciences. 2023;13(6):848.

8. Patel KR, Cherian J, Gohil K, Atkinson D. Schizophrenia: Overview and Treatment Options. 2014;
9. Haddad PM, Correll CU. The acute efficacy of antipsychotics in schizophrenia: a review of recent meta-analyses. Therapeutic Advances in Psychopharmacology. 2018;8(11):303–18.
10. Rodríguez-Sánchez JM, Crespo-Facorro B, González-Blanch C, Pérez-Iglesias R, Vázquez-Barquero JL, PAFIP Group Study. Cognitive dysfunction in first-episode psychosis: the processing speed hypothesis. Br J Psychiatry. 2007;191(S51):s107–10.
11. McCutcheon RA, Reis Marques T, Howes OD. Schizophrenia—An Overview. JAMA Psychiatry. 2020;77(2):201.
12. Crespo-Facorro B, Such P, Nylander AG, Madera J, Resemann HK, Worthington E, et al. The burden of disease in early schizophrenia – a systematic literature review. Current Medical Research and Opinion. 2021;37(1):109–21.
13. Patel SJ, Khan S, M S, Hamid P. The Association Between Cannabis Use and Schizophrenia: Causative or Curative? A Systematic Review. Cureus [Internet]. 2020 Jul 21 [cited 2023 Nov 6]; Available from: https://www.cureus.com/articles/36042-the-association-between-cannabis-use-and-schizophrenia-causative-or-curative-a-systematic-review
14. Martín-Cuevas C, Ramos-Herrero VD, Crespo-Facorro B, Sánchez-Hidalgo AC. Prenatal risk factors and postnatal cannabis exposure: Assessing dual models of schizophrenia-like rodents. Neuroscience & Biobehavioral Reviews. 2023;154:105409.
15. Guerrin CGJ, Doorduin J, Sommer IE, De Vries EFJ. The dual hit hypothesis of schizophrenia: Evidence from animal models. Neuroscience & Biobehavioral Reviews. 2021;131:1150–68.
16. MacDowell KS, Munarriz-Cuezva E, Caso JR, Madrigal JLM, Zabala A, Meana JJ, et al. Paliperidone reverts Toll-like receptor 3 signaling pathway activation and cognitive deficits in a maternal immune activation mouse model of schizophrenia. Neuropharmacology. 2017;116:196–207.
17. Suárez-Pinilla P, López-Gil J, Crespo-Facorro B. Immune system: A possible nexus between cannabinoids and psychosis. Brain, Behavior, and Immunity. 2014;40:269–82.
18. Setién-Suero E, Suárez-Pinilla P, Ferro A, Tabarés-Seisdedos R, Crespo-Facorro B, Ayesa-Arriola R. Childhood trauma and substance use underlying psychosis: a systematic review. European Journal of Psychotraumatology. 2020;11(1):1748342.
19. Hall MB, Willis DE, Rodriguez EL, Schwarz JM. Maternal immune activation as an epidemiological risk factor for neurodevelopmental disorders: Considerations of timing, severity, individual differences, and sex in human and rodent studies. Front Neurosci. 2023;17:1135559.
20. Bayer TA, Falkai P, Maier W. Genetic and non-genetic vulnerability factors in schizophrenia: the basis of the “Two hit hypothesis.” Journal of Psychiatric Research. 1999;33(6):543–8.
21. Guma E, Plitman E, Chakravarty MM. The role of maternal immune activation in altering the neurodevelopmental trajectories of offspring: A translational review of neuroimaging studies with implications for autism spectrum disorder and schizophrenia. Neuroscience & Biobehavioral Reviews. 2019;104:141–57.

22. Bauman MD, Van De Water J. Translational opportunities in the prenatal immune environment: Promises and limitations of the maternal immune activation model. Neurobiology of Disease. 2020;141:104864.
23. Han VX, Patel S, Jones HF, Nielsen TC, Mohammad SS, Hofer MJ, et al. Maternal acute and chronic inflammation in pregnancy is associated with common neurodevelopmental disorders: a systematic review. Transl Psychiatry. 2021;11(1):71.
24. Lecca S, Luchicchi A, Scherma M, Fadda P, Muntoni AL, Pistis M. Δ9-Tetrahydrocannabinol During Adolescence Attenuates Disruption of Dopamine Function Induced in Rats by Maternal Immune Activation. Front Behav Neurosci. 2019;13:202.
25. Guma E, Cupo L, Ma W, Gallino D, Moquin L, Gratton A, et al. Investigating the “two-hit hypothesis”: Effects of prenatal maternal immune activation and adolescent cannabis use on neurodevelopment in mice. Progress in Neuro-Psychopharmacology and Biological Psychiatry. 2023;120:110642.
26. Murlanova K, Pletnikov MV. Modeling psychotic disorders: Environment x environment interaction. Neuroscience & Biobehavioral Reviews. 2023;152:105310.
27. Malaspina D. Interaction of genes and prenatal exposures in schizophrenia..), Prenatal exposures in schizophrenia. 1999;American Psychiatric Association:(pp. 35–59).
28. Haddad FL, Patel SV, Schmid S. Maternal Immune Activation by Poly I:C as a preclinical Model for Neurodevelopmental Disorders: A focus on Autism and Schizophrenia. Neuroscience & Biobehavioral Reviews. 2020;113:546–67.
29. Sánchez-Hidalgo AC, Martín-Cuevas C, Crespo-Facorro B, Garrido-Torres N. Reelin Alterations, Behavioral Phenotypes, and Brain Anomalies in Schizophrenia: A Systematic Review of Insights From Rodent Models. Front Neuroanat. 2022;16:844737.
30. Lamanna-Rama N, Romero-Miguel D, Casquero-Veiga M, MacDowell KS, Santa-Marta C, Torres-Sánchez S, et al. THC improves behavioural schizophrenia-like deficits that CBD fails to overcome: a comprehensive multilevel approach using the Poly I:C maternal immune activation. Psychiatry Research. 2024;331:115643.
31. Johnson-Ferguson L, Di Forti M. From heavy cannabis use to psychosis: is it time to take action? Ir j psychol Med. 2023;40(1):13–8.
32. Abush H, Ghose S, Van Enkevort EA, Clementz BA, Pearlson GD, Sweeney JA, et al. Associations between adolescent cannabis use and brain structure in psychosis. Psychiatry Research: Neuroimaging. 2018;276:53–64.
33. Chesworth R, Karl T. Molecular Basis of Cannabis-Induced Schizophrenia-Relevant Behaviours: Insights from Animal Models. Curr Behav Neurosci Rep. 2017;4(3):254–79.
34. Wasser CR, Herz J. Reelin: Neurodevelopmental Architect and Homeostatic Regulator of Excitatory Synapses. Journal of Biological Chemistry. 2017;292(4):1330–8.
35. Marzan S, Aziz MdA, Islam MS. Association Between REELIN Gene Polymorphisms (rs7341475 and rs262355) and Risk of Schizophrenia: an Updated Meta-analysis. J Mol Neurosci. 2021;71(4):675–90.

36. Alexander A, Herz J, Calvier L. Reelin through the years: From brain development to inflammation. Cell Reports. 2023;42(6):112669.
37. Yamakage Y, Kato M, Hongo A, Ogino H, Ishii K, Ishizuka T, et al. A disintegrin and metalloproteinase with thrombospondin motifs 2 cleaves and inactivates Reelin in the postnatal cerebral cortex and hippocampus, but not in the cerebellum. Molecular and Cellular Neuroscience. 2019;100:103401.
38. Jossin Y. Reelin Functions, Mechanisms of Action and Signaling Pathways During Brain Development and Maturation. Biomolecules. 2020;10(6):964.
39. Bosch C, Masachs N, Exposito-Alonso D, Martínez A, Teixeira CM, Fernaud I, et al. Reelin Regulates the Maturation of Dendritic Spines, Synaptogenesis and Glial Ensheathment of Newborn Granule Cells. Cereb Cortex. 2016;26(11):4282–98.
40. Ogino H, Hisanaga A, Kohno T, Kondo Y, Okumura K, Kamei T, et al. Secreted Metalloproteinase ADAMTS-3 Inactivates Reelin. J Neurosci. 2017;37(12):3181–91.
41. Jossin Y, Gui L, Goffinet AM. Processing of Reelin by Embryonic Neurons Is Important for Function in Tissue But Not in Dissociated Cultured Neurons. J Neurosci. 2007;27(16):4243–52.
42. Jossin Y, Ignatova N, Hiesberger T, Herz J, Lambert De Rouvroit C, Goffinet AM. The Central Fragment of Reelin, Generated by Proteolytic Processing *In Vivo*, Is Critical to Its Function during Cortical Plate Development. J Neurosci. 2004;24(2):514–21.
43. Hattori M, Kohno T. Regulation of Reelin functions by specific proteolytic processing in the brain. The Journal of Biochemistry. 2021;169(5):511–6.
44. Howell KR, Pillai A. Long-Term Effects of Prenatal Hypoxia on Schizophrenia-Like Phenotype in Heterozygous Reeler Mice. Mol Neurobiol. 2016;53(5):3267–76.
45. Ovadia G, Shifman S. The Genetic Variation of RELN Expression in Schizophrenia and Bipolar Disorder. Burne T, editor. PLoS ONE. 2011;6(5):e19955.
46. Lidón L, Urrea L, Llorens F, Gil V, Alvarez I, Diez-Fairen M, et al. Disease-Specific Changes in Reelin Protein and mRNA in Neurodegenerative Diseases. Cells. 2020;9(5):1252.
47. Valderrama-Mantilla AI, Martín-Cuevas C, Gómez-Garrido A, Morente-Montilla C, Crespo-Facorro B, García-Cerro S. Shared molecular signature in Alzheimer's disease and schizophrenia: A systematic review of the reelin signaling pathway. Neuroscience & Biobehavioral Reviews. 2025;169:106032.
48. Fatemi SH, Emamian ES, Sidwell RW, Kist DA, Stary JM, Earle JA, et al. Human influenza viral infection in utero alters glial fibrillary acidic protein immunoreactivity in the developing brains of neonatal mice. Mol Psychiatry. 2002;7(6):633–40.
49. Reisinger S, Khan D, Kong E, Berger A, Pollak A, Pollak DD. The Poly(I:C)-induced maternal immune activation model in preclinical neuropsychiatric drug discovery. Pharmacology & Therapeutics. 2015;149:213–26.
50. Meyer U, Nyffeler M, Engler A, Urwyler A, Schedlowski M, Knuesel I, et al. The Time of Prenatal Immune Challenge Determines the Specificity of Inflammation-Mediated Brain and Behavioral Pathology. J Neurosci. 2006;26(18):4752–62.

51. Munarriz-Cuezva E, Meana JJ. Poly (I:C)-induced maternal immune activation generates impairment of reversal learning performance in offspring. Journal of Neurochemistry. 2025;169(1):e16212.
52. Mueller FS, Richetto J, Hayes LN, Zambon A, Pollak DD, Sawa A, et al. Influence of poly(I:C) variability on thermoregulation, immune responses and pregnancy outcomes in mouse models of maternal immune activation. Brain, Behavior, and Immunity. 2019;80:406–18.
53. Rogers DC, Fisher EMC, Brown SDM, Peters J, Hunter AJ, Martin JE. Behavioral and functional analysis of mouse phenotype: SHIRPA, a proposed protocol for comprehensive phenotype assessment. Mammalian Genome. 1997;8(10):711–3.
54. Glaser EM, Van Der Loos H. Analysis of thick brain sections by obverse—Reverse computer microscopy: Application of a new, high clarity Golgi—Nissl stain. Journal of Neuroscience Methods. 1981;4(2):117–25.
55. Harte LC, Dow-Edwards D. Sexually dimorphic alterations in locomotion and reversal learning after adolescent tetrahydrocannabinol exposure in the rat. Neurotoxicology and Teratology. 2010;32(5):515–24.
56. Kasten CR, Zhang Y, Boehm SL. Acute Cannabinoids Produce Robust Anxiety-Like and Locomotor Effects in Mice, but Long-Term Consequences Are Age- and Sex-Dependent. Front Behav Neurosci. 2019;13:32.
57. Morrens M, Hulstijn W, Lewi PJ, De Hert M, Sabbe BGC. Stereotypy in schizophrenia. Schizophrenia Research. 2006;84(2–3):397–404.
58. Schwartzer JJ, Careaga M, Onore CE, Rushakoff JA, Berman RF, Ashwood P. Maternal immune activation and strain specific interactions in the development of autism-like behaviors in mice. Transl Psychiatry. 2013;3(3):e240–e240.
59. Lan XY, Gu YY, Li MJ, Song TJ, Zhai FJ, Zhang Y, et al. Poly(I:C)-induced maternal immune activation causes elevated self-grooming in male rat offspring: Involvement of abnormal postpartum static nursing in dam. Front Cell Dev Biol. 2023;11:1054381.
60. Prashad S, Filbey FM. Cognitive motor deficits in cannabis users. Current Opinion in Behavioral Sciences. 2017;13:1–7.
61. Hitchcock LN, Tracy BL, Bryan AD, Hutchison KE, Bidwell LC. Acute Effects of Cannabis Concentrate on Motor Control and Speed: Smartphone-Based Mobile Assessment. Front Psychiatry. 2021;11:623672.
62. Kirschmann EK, Pollock MW, Nagarajan V, Torregrossa MM. Effects of Adolescent Cannabinoid Self-Administration in Rats on Addiction-Related Behaviors and Working Memory. Neuropsychopharmacol. 2017;42(5):989–1000.
63. Ratnayake U, Quinn TA, Castillo-Melendez M, Dickinson H, Walker DW. Behaviour and hippocampus-specific changes in spiny mouse neonates after treatment of the mother with the viral-mimetic Poly I:C at mid-pregnancy. Brain, Behavior, and Immunity. 2012;26(8):1288–99.
64. Gray A, Tattoli R, Dunn A, Hodgson DM, Michie PT, Harms L. Maternal immune activation in mid-late gestation alters amphetamine sensitivity and object recognition, but not other schizophrenia-related

behaviours in adult rats. Behavioural Brain Research. 2019;356:358–64.

65. Nenadic I, Yotter RA, Sauer H, Gaser C. Patterns of cortical thinning in different subgroups of schizophrenia. Br J Psychiatry. 2015;206(6):479–83.
66. Yan J, Cui Y, Li Q, Tian L, Liu B, Jiang T, et al. Cortical thinning and flattening in schizophrenia and their unaffected parents. NDT. 2019;Volume 15:935–46.
67. Smith SEP, Elliott RM, Anderson MP. Maternal Immune Activation Increases Neonatal Mouse Cortex Thickness and Cell Density. J Neuroimmune Pharmacol. 2012;7(3):529–32.
68. Baines KJ, Hillier DM, Haddad FL, Rajakumar N, Schmid S, Renaud SJ. Maternal Immune Activation Alters Fetal Brain Development and Enhances Proliferation of Neural Precursor Cells in Rats. Front Immunol. 2020;11:1145.
69. Vlasova RM, Iosif AM, Ryan AM, Funk LH, Murai T, Chen S, et al. Maternal Immune Activation during Pregnancy Alters Postnatal Brain Growth and Cognitive Development in Nonhuman Primate Offspring. J Neurosci. 2021;41(48):9971–87.
70. Rais M, Van Haren NEM, Cahn W, Schnack HG, Lepage C, Collins L, et al. Cannabis use and progressive cortical thickness loss in areas rich in CB1 receptors during the first five years of schizophrenia. European Neuropsychopharmacology. 2010;20(12):855–65.
71. Manza P, Yuan K, Shokri-Kojori E, Tomasi D, Volkow ND. Brain structural changes in cannabis dependence: association with MAGL. Mol Psychiatry. 2020;25(12):3256–66.
72. Mashhoon Y, Sava S, Sneider JT, Nickerson LD, Silveri MM. Cortical thinness and volume differences associated with marijuana abuse in emerging adults. Drug and Alcohol Dependence. 2015;155:275–83.
73. Ayesa-Arriola R, De La Foz VOG, Setién-Suero E, Ramírez-Bonilla ML, Suárez-Pinilla P, Son JM van, et al. Understanding sex differences in long-term outcomes after a first episode of psychosis. npj Schizophr. 2020;6(1):33.
74. Estes ML, McAllister AK. Maternal immune activation: Implications for neuropsychiatric disorders. Science. 2016;353(6301):772–7.
75. Gumusoglu SB, Stevens HE. Maternal Inflammation and Neurodevelopmental Programming: A Review of Preclinical Outcomes and Implications for Translational Psychiatry. Biological Psychiatry. 2019;85(2):107–21.
76. Smith-Osborne L, Duong A, Resendez A, Palme R, Fadok JP. Female dominance hierarchies influence responses to psychosocial stressors. Current Biology. 2023;33(8):1535–1549.e5.
77. Karamihalev S, Brivio E, Flachskamm C, Stoffel R, Schmidt MV, Chen A. Social dominance mediates behavioral adaptation to chronic stress in a sex-specific manner. eLife. 2020;9:e58723.
78. Williamson CM, Lee W, DeCasien AR, Lanham A, Romeo RD, Curley JP. Social hierarchy position in female mice is associated with plasma corticosterone levels and hypothalamic gene expression. Sci Rep. 2019;9(1):7324.

79. Van Den Berg WE, Lamballais S, Kushner SA. Sex-Specific Mechanism of Social Hierarchy in Mice. Neuropsychopharmacol. 2015;40(6):1364–72.
80. Gillespie B, Panthi S, Sundram S, Hill RA. The impact of maternal immune activation on GABAergic interneuron development: A systematic review of rodent studies and their translational implications. Neuroscience & Biobehavioral Reviews. 2024;156:105488.
81. Okugawa E, Ogino H, Shigenobu T, Yamakage Y, Tsuiji H, Oishi H, et al. Physiological significance of proteolytic processing of Reelin revealed by cleavage-resistant Reelin knock-in mice. Sci Rep. 2020;10(1):4471.
82. Garey L. When cortical development goes wrong: schizophrenia as a neurodevelopmental disease of microcircuits. Journal of Anatomy. 2010;217(4):324–33.

Figures

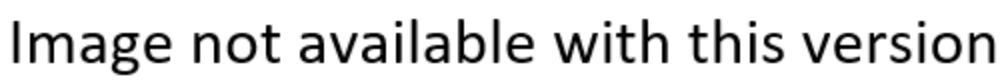


Figure 1

Graphical abstract. Abbreviations: Poly(I:C): polyinosinic-polycytidylic acid; THC: Δ9-tetrahydrocannabinol; GD: gestational day; PD: postnatal day; PFC: prefrontal cortex; HP: hippocampus. Created with Biorender.com

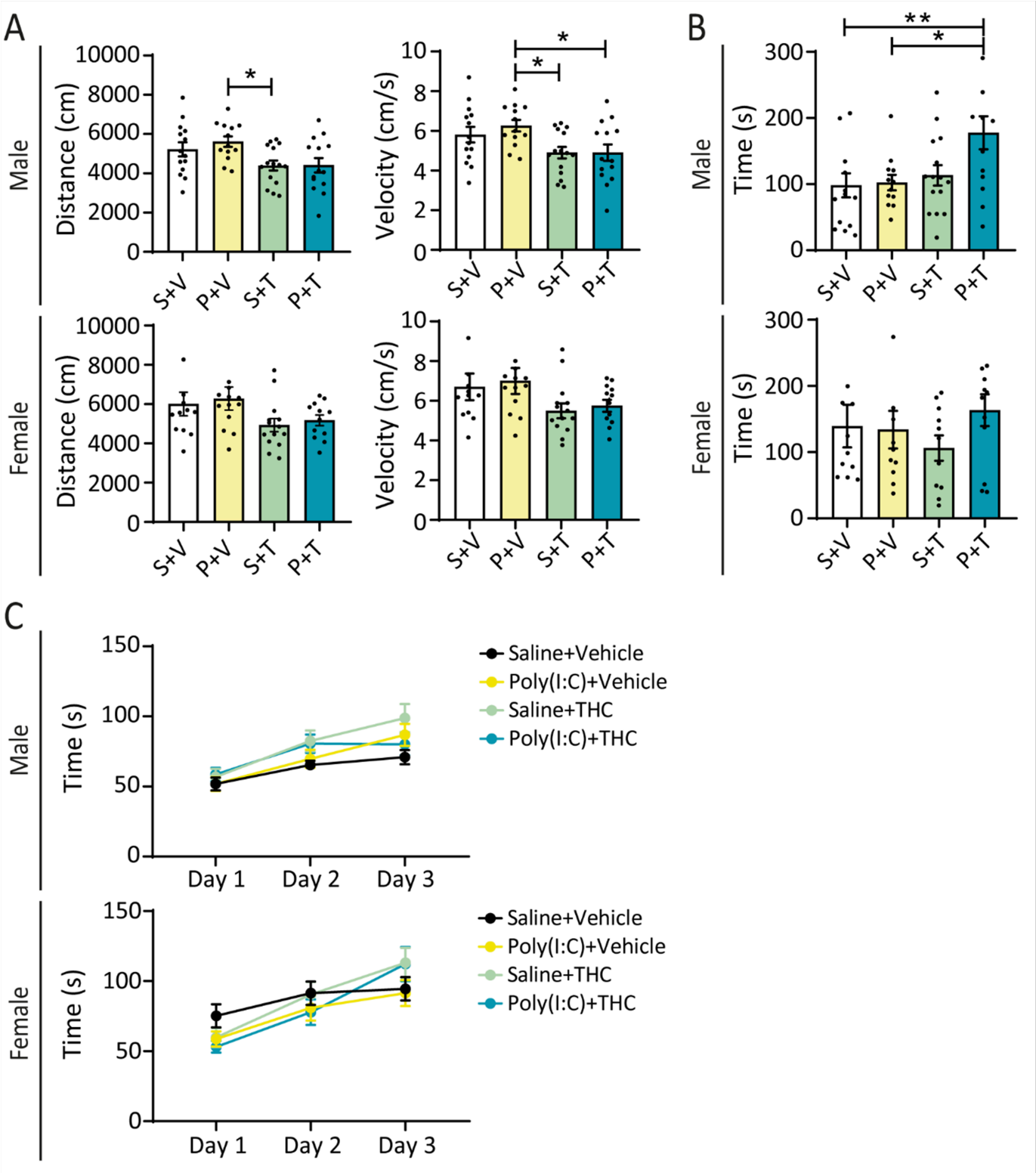


Figure 2

Poly(I:C)+THC male mice display increased stereotyped behavior. **A,** Open field test. Total distance traveled and velocity (n = 12-15 per treatment and sex) (two-way ANOVA with Tukey's post-hoc analysis; *p < 0.05). **B,** Self-grooming time (n = 12-15 per treatment and sex) (two-way ANOVA with Tukey's post-hoc analysis; *p < 0.05; **p < 0.01). **C,**Rotarod test. Latency to fall (n = 12-15 per treatment and sex)

(repeated-measures three-way ANOVA with Tukey's post-hoc analysis). Abbreviations: Saline+Vehicle (S+V), Poly(I:C)+Vehicle (P+V), Saline+THC (S+T), Poly(I:C)+THC (P+T).

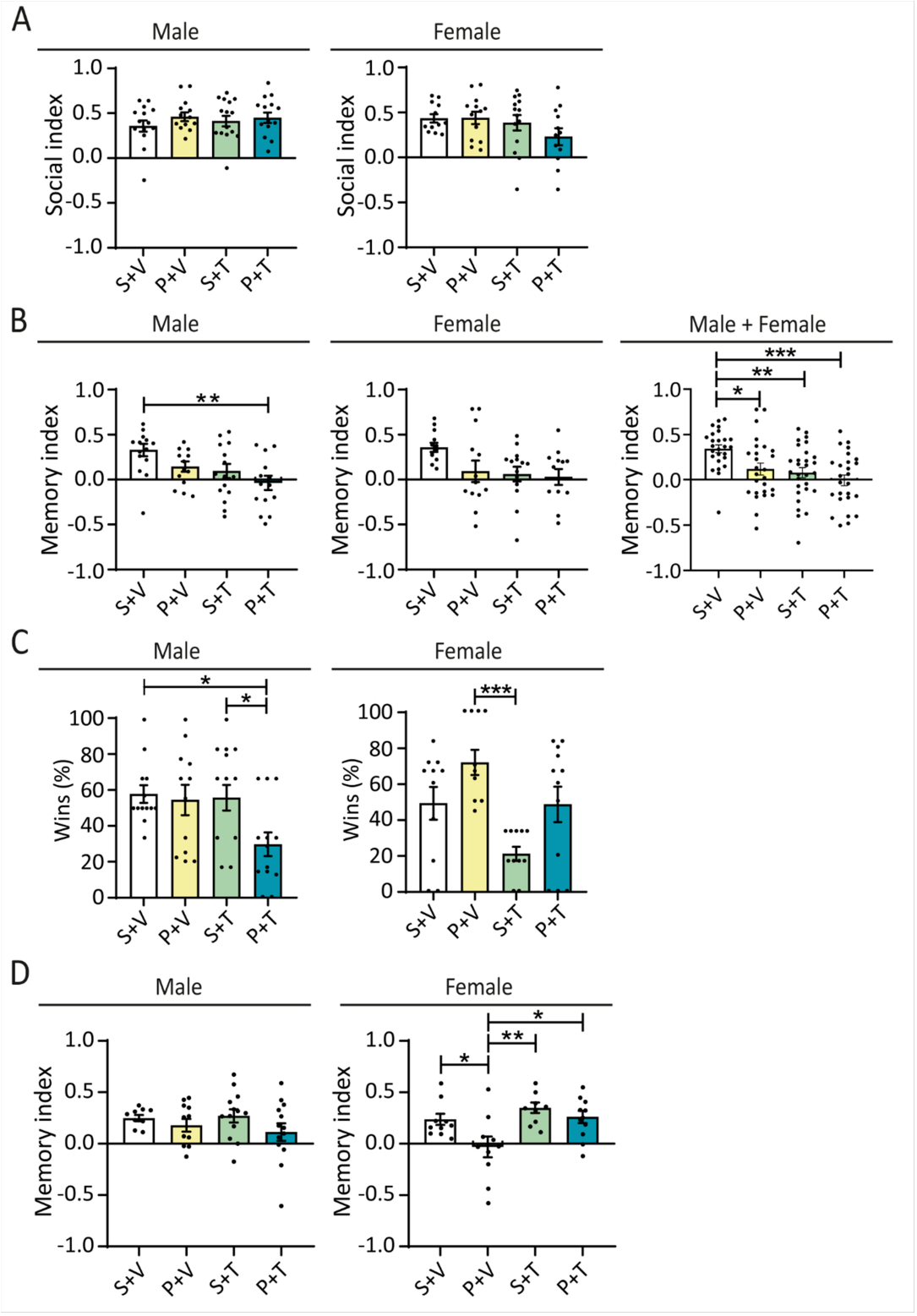


Figure 3

The dual-hit paradigm impairs social novelty in both sexes, dominance in male mice and recognition memory in female mice. **A,** Three-chamber test. Social index in the social preference phase (n = 12-15

per treatment and sex) (two-way ANOVA with Tukey's post-hoc analysis). **B,** Three-chamber test. Memory index in the social novelty phase (n = 12-15 per treatment and sex) (two-way ANOVA with Tukey's post-hoc analysis; **p < 0.01). **C,** Tube test. Percentage of wins (n = 12-15 per treatment and sex) (two-way ANOVA with Tukey's post-hoc analysis; *p < 0.05, ***p < 0.001). **D,** Novel object recognition test. Memory index (n = 12-15 per treatment and sex) (two-way ANOVA with Tukey's post-hoc analysis; *p < 0.05, **p < 0.01). Abbreviations: Saline+Vehicle (S+V), Poly(I:C)+Vehicle (P+V), Saline+THC (S+T), Poly(I:C)+THC (P+T).

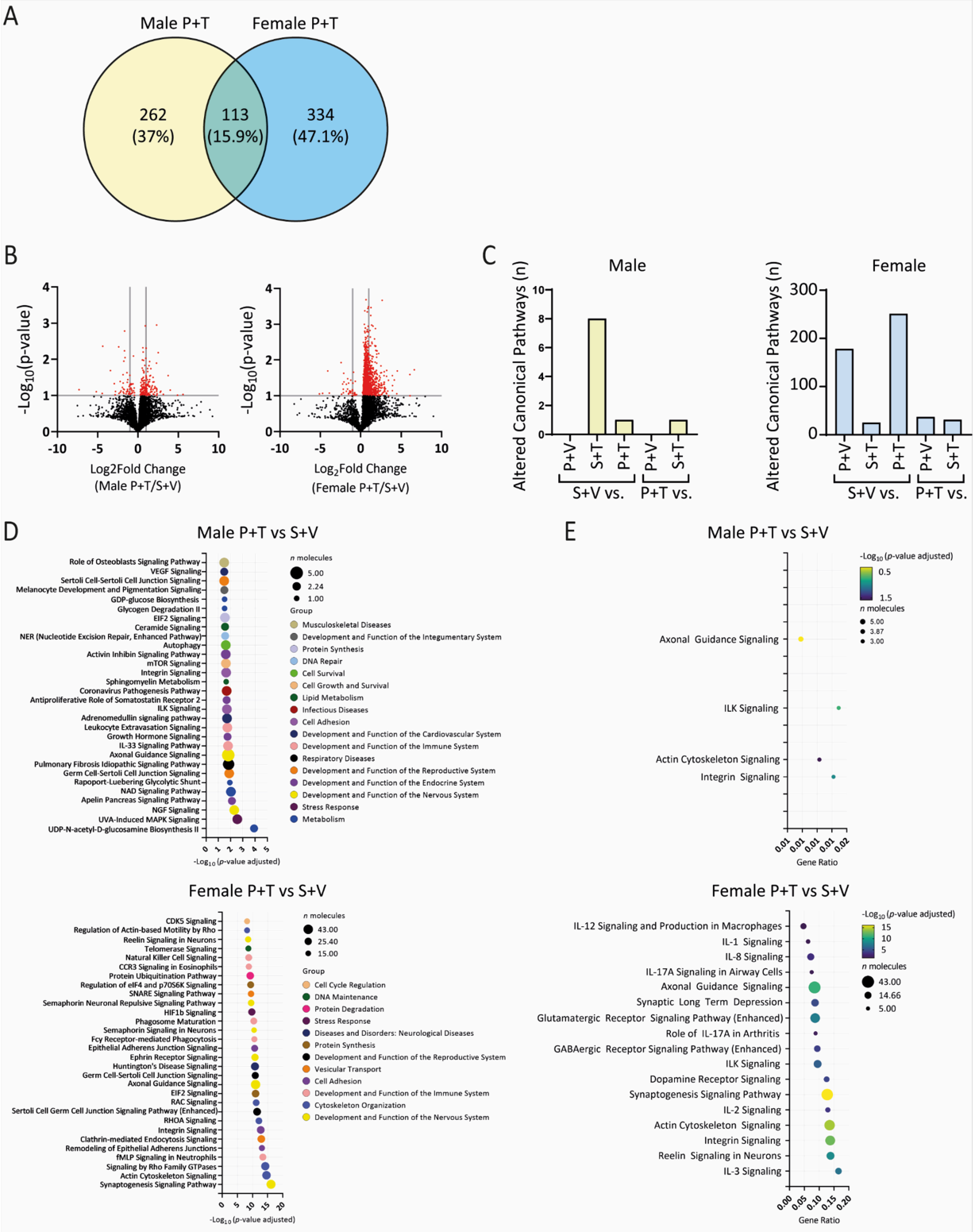


Figure 4

Quantitative proteomics analysis of PFC samples from Poly(I:C)- and/or THC-treated mice. A, Venn diagram showing the number and percentage of proteins altered after Poly(I:C)+THC treatment in males (yellow) and females (blue) compared to controls, including those commonly affected in both sexes. **B,** Volcano plot illustrating the distribution of differentially expressed proteins based on log2(Fold Change) and -log10(p-value) for the Poly(I:C)+THC male vs. Poly(I:C)+THC female comparison, normalized to their respective controls. Proteins with significant differential expression ($p < 0.05$) are highlighted in red. **C,** Count of significantly altered canonical pathways ($p < 0.05$) identified in each indicated comparison for males and females. **D,** Ingenuity Canonical Pathways enrichment analysis depicting significantly differentially expressed pathways in Poly(I:C)+THC-treated males (upper panel) and females (bottom panel), normalized to their respective controls. Dot size corresponds to the number of altered proteins within each pathway (n molecules). **E,** Dot plot quantifying the number of significantly altered proteins per pathway set and the total dataset (Gene Ratio) in males (upper panel) and females (bottom panel), normalized to their respective controls. Color intensity represents the adjusted p-value (-log10), while dot size indicates the number of altered proteins within each pathway. Abbreviations: Saline+Vehicle (S+V), Poly(I:C)+Vehicle (P+V), Saline+THC (S+T), Poly(I:C)+THC (P+T).

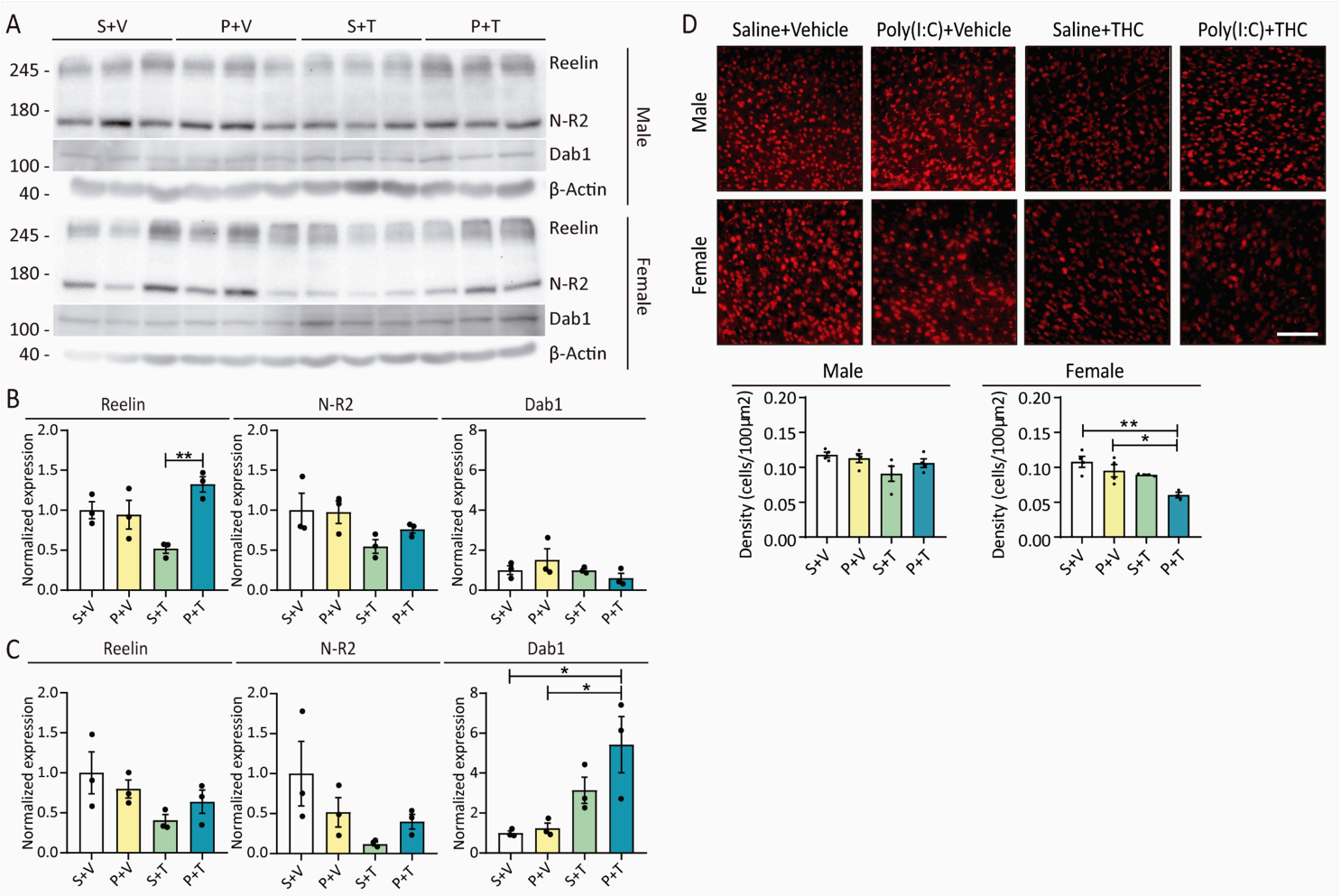


Figure 5

Reelin and Dab1 expression are altered in the model. **A,** Western blot experiments from PFC lysates of S+V, P+V, S+T and P+T male and female mice. **B,** Normalized expression of Reelin, N-R2 fragment and Dab1 (male mice) (two-way ANOVA with Tukey's post-hoc analysis; **p < 0.01). **C,** Normalized expression of Reelin, N-R2 fragment and Dab1 (female mice) (two-way ANOVA with Tukey's post-hoc analysis) (n = 3 per treatment and sex). **D,**Reelin+ cell density is reduced in the dual-hit mice (two-way ANOVA with Tukey's post-hoc analysis; *p < 0.05; **p < 0.01) (n = 3-4 per treatment and sex). Scale: 180μm. Abbreviations: Saline+Vehicle (S+V), Poly(I:C)+Vehicle (P+V), Saline+THC (S+T), Poly(I:C)+THC (P+T).

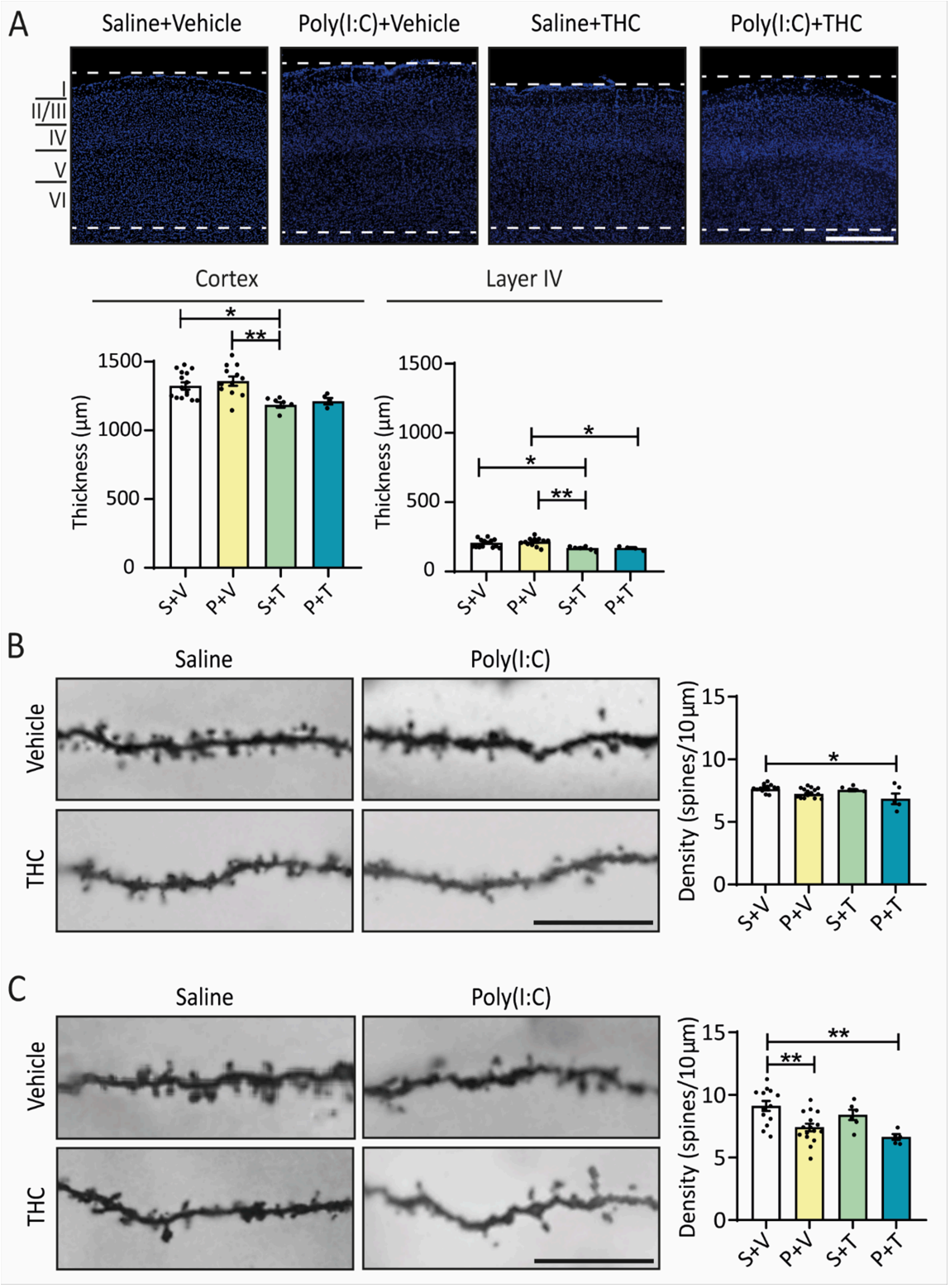


Figure 6

Total cortical thickness is reduced by THC treatment and Poly(I:C)+THC treatment causes a decreased dendritic spine density in PFC and HP. **A,** Total cortical thickness (total cortex and layer IV) (n = 4-15 per treatment) (two-way ANOVA with Tukey's post-hoc analysis; *p < 0.05, **p<0.01). Scale: 500µm. **B,** Dendritic spine density in CA1 (HP) (n = 5-16 per treatment) (two-way ANOVA with Tukey's post-hoc analysis; *p < 0.05). Scale: 10µm. **C,** Dendritic spine density in PFC (n = 5-16 per treatment) (two-way

ANOVA with Tukey’s post-hoc analysis; **p < 0.01). Scale: 10μm. Abbreviations: Saline+Vehicle (S+V), Poly(I:C)+Vehicle (P+V), Saline+THC (S+T), Poly(I:C)+THC (P+T).

Supplementary Files

This is a list of supplementary files associated with this preprint. Click to download.

- Summaryforsupplementarymaterial.docx
- Supplementarymaterial1.pdf
- Supplementarymaterial2.xlsx
- Supplementarymaterial3.xlsx
- Supplementarymaterial4.xlsx